

11-27-2020

## Effect of Operational Parameters on Three-Phase Air-Lift Pump Performance.

M. Hosien

*Department of Mechanical power Engineering, Faculty of Engineering Minoufiya University, Shebin El-Kom, Egypt*

S. Selim

*Department of Mechanical power Engineering, Faculty of Engineering Minoufiya University, Shebin El-Kom, Egypt*

Follow this and additional works at: <https://mej.researchcommons.org/home>

---

### Recommended Citation

Hosien, M. and Selim, S. (2020) "Effect of Operational Parameters on Three-Phase Air-Lift Pump Performance.," *Mansoura Engineering Journal*: Vol. 34 : Iss. 2 , Article 28.

Available at: <https://doi.org/10.21608/bfemu.2020.126200>

This Original Study is brought to you for free and open access by Mansoura Engineering Journal. It has been accepted for inclusion in Mansoura Engineering Journal by an authorized editor of Mansoura Engineering Journal. For more information, please contact [mej@mans.edu.eg](mailto:mej@mans.edu.eg).

## EFFECT OF OPERATIONAL PARAMETERS ON THREE-PHASE AIR-LIFT PUMP PERFORMANCE

تأثير المعايير التشغيلية على أداء مضخات رفع الهواء للسريان ثلاثي الطور

M.A.Hosien\* and S.M.Selim\*\*

Department of Mechanical power Engineering, Faculty of Engineering  
Minoufiya University, Shebin El -Kom, Egypt

المضخة الرافعة بالهواء هي نوع من أنواع مضخات الآبار العميقة و يمكن استعمالها أحيانا لإزالة المياه من المناجم أو لضخ الطين السائل من الرمل و الماء أو المحاليل الأخرى. يعتمد أداء مضخات الرفع بالهواء بشكل رئيسي على المعايير التشغيلية مثل التدفق الحجمي للهواء، وطبيعة الماء و المادة الصلبة المرغوة. الهدف الرئيسي لهذا العمل هو دراسة أداء مضخة الرفع بالهواء نظرياً تحت عدد من ظروف التشغيل. ولقد تم تطوير نموذج رياضي لمحاكاة أداء مضخة الرفع بالهواء، وقد أخذت المعايير التشغيلية في الاعتبار. كما تم تطوير برنامج حاسوب لحل معادلة كمية التحرك الخاصة بالنموذج الرياضي. و تمت مقارنة نتائج النموذج بالبيانات المنشورة المتوفرة. وكان هناك توافق جيد بين النتائج الحالية و البيانات المنشورة. و تم التنبؤ بتأثيرات المعايير التشغيلية على أداء المضخة الرافعة بالهواء و سجلت بياناتاً مقابل التدفق الحجمي للماء و كفاءة المضخة. ولقد أظهرت النتائج أن التدفق الحجمي للماء وكفاءة المضخة تزيد بالتدرج حتى أقصى قيمة ما بين 1 إلى 4 متر/ الثانية ثم تقل تدريجياً بزيادة معدل التدفق الحجمي للهواء. كما ان معدل تدفق المياه الحجمي وكفاءة المضخة يقل خطياً بزيادة التدفق الحجمي للجسيمات الصلبة. بينت النتائج أيضاً ان كثافة الجسيمات الصلبة وقطرها له أثر ضعيف على أداء المضخة.

### ABSTRACT

Air-lift pump is a type of deep wells pumps. Sometimes, it can be used for removing water from mines or to pump slurry of sand and water or other solutions. The performance of air-lift pumps depends mainly on the operational parameters such as air volumetric flux, nature of lifted water and solid. The main objective of the present work is to study theoretically the air-lift pump performance under variety of operational parameters. A mathematical model simulating the performance of air-lift pump under various operational parameters was developed. A computer program was developed to solve the governing equation. The model results were compared with available published data for validation. There was a good agreement between the present results and the published data. The effects of operational parameters on the air-lift pump performance are predicated and plotted against the water volumetric flux and pump efficiency. The results showed that the water volumetric flux and pump efficiency increased gradually reaching a maximum value some where between 1 to 4  $m/s$ , then slightly decrease with increasing the air volumetric flux. The water volumetric flux and pump efficiency decrease linearly with increasing the solid particles volumetric flux. The predicted results show that the solid particles density and diameter had slight effects on the pump performance.

Key Words: Air-lift pump, Solid particles, Submergence ratio, Slug flow, Churn flow, – Bubbly flow, Three-phase flow.

\* Lecturer \*\* Professor

## 1. INTRODUCTION

The simplicity in construction and absence of moving mechanical parts are two very important advantages that makes the air-lift pump useful in certain applications, where reciprocating and centrifugal pumps cannot be used. It can be used to pump water from boreholes of any diameter and depth and are the most simple and reliable devices to serve this purpose, sometimes used to remove water from mines. The great focus towards the renewable energy for water pumping applications brought the attention to revisit the analysis of the air-lift pump. In simple air-lift pumping system the wind turbine drives an air compressor which supplies an air-lift pump submerged in the well, or fluid source. It is possible to locate the turbine/compressor unit remotely from the site. Air-lift pumps can be used to pump liquids contaminated by sand ash, or peat or other "gritty" solutions and also used in nautical archaeology to suck small objects, sand and mud from the sea bed and to transport the resulting debris upwards and away from its source. Air-lift pumps are, usually used for difficult pumping operations, such as underwater explorations for lifting marine mineral resources such as manganese nodules from the deep-sea bed at about 4000-6000 m to the sea surface, (Hatta et al. (1998)), and to raise coarse particle suspensions in the dredging of river estuaries and harbors. Recently, air lift pumps have been used for pumping boiling liquids where there is a change in phase from liquid to gas; and in petroleum fields, gas-lift pumps are used for raising oil from weak wells, (Brown and Heywood (1991), Khalil et al. (1999), Hatta et al. (1998) and Dedegil, (1986)). Use of air-lift pump as the Defense Waste Processing Facility (DWPF), successfully operated and provided sufficient flow to pump glass from the

bottom of the melt pool without excessive glass foaming, (Imrich et al. (2004)).

Kato et al. (1975) investigated experimentally and analytically the performance of low head air-lift pumps used to lift particles. The pump was analyzed based on an existing theory of two-phase flow. The model was developed by coupling the momentum equation of two-phase flow and the equation of motion of a single solid particle. The riser tube used was transparent glass pipe and solid particles were glass balls with different diameters. Tests were carried out in the three-phase flow section by independently changing the flow rates of air, water and solid particle. The experimental and analytical results were found to be in acceptable agreement. Wurts et al. (1994) conducted experiments on air-lift pumps characteristics at various riser diameters. Air was injected at different positions below the discharge outlet with varied flow rates. Their results showed that air-lift pumping rates increased as the air flow increased. Yoshinaga and Sato (1996) carried out an extensive experimental study in order to investigate the performance of an air-lift pump used for conveying uniform coarse particles. The experiments performed using ceramic spheres with different densities as solid particles, water and air as the working fluids. The experiments were examined with two air-lift pumps of same height but, different tube diameter and various submergence ratios. Also they proposed a theoretical analysis, to predict the air-lift pump performance, based on the concept of momentum balance. The validity of that approach was confirmed with the experimental data of other investigators as well as with their own experimental data. It was seen that the theoretical model developed by this method was valid

not only for relatively small-scale air-lift pumps but also for relatively large and tall ones of about 300 mm in diameter and 250 m height. Hatta et al. (1998) proposed a method for predicting the efficiency of an air-lift pump based on one-dimensional multi-fluid model. The multi-fluid model was formulated by a set of conservation equation governing balance of mass and momentum of different phases in each section of the air-lifting pipe. Steady-state flow characteristics were predicated by solving the system of equations numerically with the aid of Euler method. The predictions were compared with the experiments conducted by other researchers for validation. Comparison showed that the theoretical model built up in the study gave best-fit to the prediction of the operation performance of an air-lift pump data of other investigators. They conducted that the theoretical model on the basis of the multi -fluid model was capable of predicting the maximum solid/liquid volumetric flux. Kandil and Elmiligui (1998) conducted an experimental investigation of the performance of air-lift pump lifting coarse, irregular and non-uniform solid particles, and sand particles under various submergence ratios. They concluded that the performance of the pump was greatly affected by the submergence ratio where the flow rate of solid particles increased with increasing the submergence ratio at a constant flow rate. Also, there was always a point of maximum flow rate beyond which the flow rate dropped slightly. Kassab et al. (2001) carried out experimentall investigation to obtain the performance of an air-lift pump lifting coarse, irregular solid particles. The pump performance was obtained using crushed pink limestone. The performance of the pump was studied under various submergence ratios. The experimental results

indicated that the solid mass flow rate increased with the increase of the submergence ratio and/or the decrease of the particle size. The performance of air-lift pump, lifting water and solid particles, depended on the flow pattern in which the pump operates. The air-lift pump operated in the slug or slug-churn regime gives maximum water and solid mass flow rates. Abed (2003) conducted a theoretical analysis using the model of Stenning and Martin (1968) with the modification suggested by Parker (1980) to find operating characteristics curves of air-lift pumps at wide range of operating conditions and the operating limits of each type. The maximum water flow rate and the corresponding air flow rate, and the minimum air flow rate needed to start the water discharge were obtained. The flow was considered two-phase and slug flow. It was concluded that, the maximum air flow rate supplied increased when inner diameter increased and submergence ratio decreased. Moreover the maximum air flow rate supplied depended on the riser tube length, submergence ratio and inner diameter of the riser. Fujimoto et al. (2003) carried out an experimental investigation of the performance of small air-lift pump for conveying solid particles. The experiments performed using alumina or glass as solid particles with different particle diameters. The flows in the lifting pipe were water/solid two-phase mixtures below the gas injection point, and air/water/solid three-phase mixtures above it. The supplied gas flux, gas injection point, particle size, and material density of particles were systematically changed as parameters. Also, the critical boundary at which the solid particles can be lifted along the pipe was studied. Results indicated that the discharged water increased with gas flux reaches a minimum value and

then decrease. The amount of discharged particles decreased with increasing particle diameter and/or density. Both the discharged water and particles become smaller for higher gas injection points. It was confirmed that the simple theoretical model, to obtain the critical boundary at which solid particle can be lifted was sufficiently predict the minimum discharged water flux. Fujimoto et al. (2004) carried out experiments to investigate the performance of a small air-lift pump for conveying solid particles. Alumina used as a solid particles. Three type of critical condition for transporting a solid particle were measured. Results indicated that the water flux for three-phase flow was essentially less than that for the case of two-phase flow. The water flux at a given gas flux decreased with increasing flux of solid particles. The solid particles were lifted if the water flux was larger than the critical value. Awari et al. (2004) developed an applied air-lift model for air-water flow (two-phase flow) experimental analysis. Experiments were conducted to study the effects of various design parameters on the performance at air-lift pump under operating conditions. They conducted comparative study of the characteristic of an air-lift pump and a two-phase centrifugal pump. A computer program was developed by correlating the various influencing parameters and on the basis of the optimization of influencing variables. Their experimental results indicated that as the air pressure increased the discharge of pump increased to a certain limit. They conducted that the present model is affected to contribute more to the optimum design of the air-lift pump installation. Nevertheless, the validity of the program is under consideration and was not presented in their present work. Kassab et al (2007) modified theoretical model based on the original

model proposed by Yoshinaga and Sato (1996) to predict the air-lift pumps performance in air-water-solid three-phase flow. The effect of solid particles on the pump performance was investigated. Also the conducted experiments using coarse, irregular non-uniform crushed pink limestone particles. Their theoretical results indicated the predictions of the proposed model were in good agreement with their experimental results of an air-lift pump conveying solid particles.

It can be concluded that, the study of the air-lift pump performance is of great importance because such type of pumping system is found in a variety of practical situations. It is appeared from the literature review of the previous work that, the air lift pump performance depends mainly on the operational parameters such as air flow rate, gas pressure, and the nature of lifted phase. It is clear that, few of the previous workers tried to optimize the air-lift pump performance. Furthermore, few of them assigned the applications of such pump for lifting a mixture of liquid and solid particle. The previous theoretical analysis suffer from the fundamental weakness that a generalized model, valid for all types of flow regimes (bubbly, slug, churn and annular) encountered in the pump riser, is impossible since each type is likely to have a different scale-law. Therefore, the main objective of the present work is to propose a theoretical model to predict the three-phase air-lift pump performance operating under various operational parameters taking into account the type of flow regime exists in the upriser of the air-lift.

## 2. THEORETICAL ANALYSIS

In many systems, it is impossible to test full scale models in the laboratory and the flow in air-lift

pumps is a highly complex phenomenon involving properties of the fluid, solids and types of multi-phase flow expected in the riser of the pump. Therefore, attempts have been made to develop theoretical models to predict the performance of air-lift pumps Yoshinaga and Sato (1996), Dedegil (1986), Hatta et al. (1998), Nicklin (1963), Boes et al. (1972), Kato et al. (1975), Clark (1984a), Clark (1985), Clark and Dabolt (1986) and Weber and Dedegil (1976). However, these theoretical analyses are not really applicable to the observations of many experimentalists. Because all these theoretical analysis suffer from the fundamental weakness that a generalized equation, valid for all types of flow encountered in the pump riser is impossible since each type is likely to have a different scale-law. Therefore, the intent in this study is to establish a general equation for predicting air-lift pumps, valid for a particular, type of flow in the pump riser, and as a foundation for later theoretical refinements. Also to see how consistent this formulation is when applied to a broad band of data. This could help the air-lift pumps designer to assess the performance likely to occur in his pump at different operating conditions.

One-dimensional theoretical analysis of the performance of an air-lift pump, used for hydrau-preumatic transport solids, based on the principle of momentum balance is presented in this study. The effect of changing operational parameters such as gas flow rate, solid particles size, density and flow rate on the air lift-pump performance will be predicted. Performing the momentum balance over the whole tube length, the liquid and air flow rates are readily numerically predicted. The numerical computations are also required to account for the variation in air pressure

and flow rate throughout the pump and also for the calculations of solid, liquid, and/or air volumetric fractions throughout every section in the air-lift tube.

### 2.1. Calculation Methods and Governing Equations

In the present theoretical study, a general analysis method for three-phase flow and a design model for an air-lift pump is presented. Essentially, the model is based on the idea proposed by (Yoshinaga and Sato (1996)). They have proposed a Figure showing the outline of the mixture flow and axial pressure distribution, which is shown in Fig. (1).

The air-lift pump illustrated in Figure (1) consists of two main parts. One of them is of length ( $L_2$ ) between the bottom end and the air-injection ports while the other is an upriser pipe of length ( $L_1$ ) between the air injection ports and discharge ports. The type of flow in the suction pipe is either one-phase (liquid) or two-phase (solid-liquid) while that in the upriser either two-phase (air-liquid) or three-phase (air-liquid-solid). Fig. (1) shows the pressure gradient throughout both the suction and upriser pipes. This figure shows that the pressure gradient inside the suction and upriser pipes is different from the hydrostatic pressure gradient outside the pipes. At the steady state condition, the air-lift pumping system operates under these pressure distributions. The symbols  $E$ ,  $I$  and  $O$  in Fig. (1) denote the levels of the suction pipe inlet, the air injector and the upriser outlet, respectively.

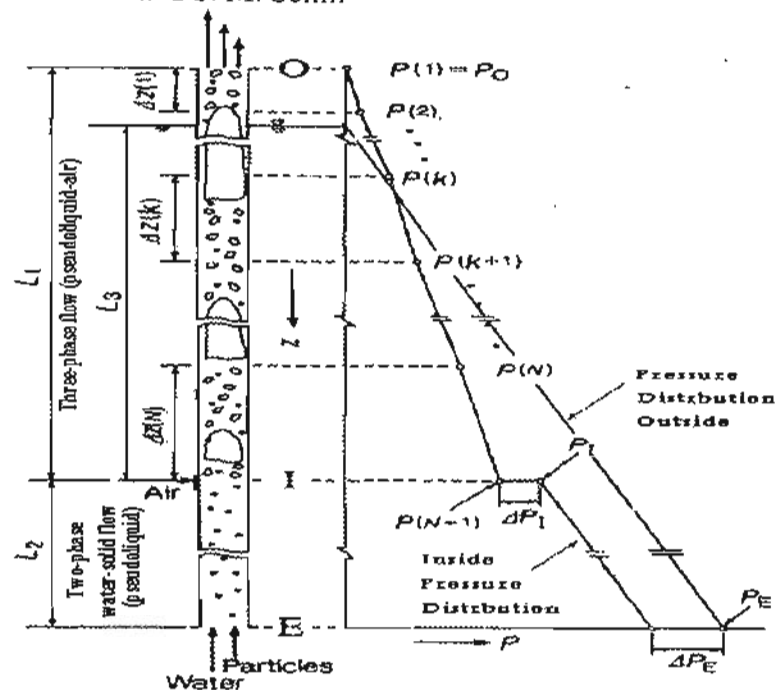


Fig. (1): Diagram of the air-lift pump and the axial pressure distribution (Yoshinaga and Sato (1996)).

### 2.1.1 Momentum equation

In the present study the following assumptions have been made for the mathematical formulation of the air-lift mechanism:

- Steady-state operating conditions,
- Compressible and ideal gas flow,
- The liquid medium is always the carrier of the solid particles,
- The place of equal velocity and equal pressure should be normal to the pipe axis. This makes the problem one-dimensional, which is approximately the case in practice,
- No change of mass or momentum between phases,
- Isothermal flow for all phase. This assumption is justified only if the three phase flow vary slowly through the pipe so that a continuous heat exchange with the environment is no longer possible,
- The solid particles are of equal size and density.

Based on the above assumptions, the governing equation representing the flow through the air-lift pump is the momentum equation. The concept

momentum will be applied to a control volume bounded by the pipe wall and the cross sections  $E$  and  $O$ . The momentum equation may therefore be written as:

$$\begin{aligned}
 & A\{\rho_L j_L u_{L,E} + \rho_S j_S u_{S,E}\} \\
 & - A\{\rho_{G,O} j_{G,O} u_{G,O} + \rho_L j_L u_{L,O} + \rho_S j_S u_{S,O}\} \\
 & - \left\{ \pi D \int_E^I \tau_{PS} dz \right\} - \left\{ \pi D \int_I^O \tau_3 dz \right\} \\
 & - \left\{ A \int_E^I (\rho_L \varepsilon_{L,PS} + \rho_S \varepsilon_{S,PS}) g dz \right\} \\
 & - \left\{ A \int_I^O (\rho_G \varepsilon_G + \rho_L \varepsilon_{L,3} + \rho_S \varepsilon_{S,3}) g dz \right\} \\
 & + \{A \rho_L g (L_2 + L_3)\} = 0 \quad (1)
 \end{aligned}$$

Where  $j$  is the volumetric flux,  $u$  is the velocity,  $\varepsilon$  is the volumetric fraction,  $\rho$  is the density,  $\tau$  is the shear stress, and  $g$  is the gravitational acceleration. The subscripts  $G$ ,  $L$ ,  $S$ ,  $PS$  and  $3$  denote the air, water, solid, two-phase water-solid mixture (treated as a single phase as pseudoliquid) and three-phase air-water-solid mixture (treated as a two-phase as air-pseudoliquid mixture), respectively. The subscripts  $E$ ,  $I$  and  $O$

represent the cross sections of the inlet, air injector and the outlet, respectively. The first and second terms in equation (1) denote the momentum which enters through  $E$  and leaves through  $O$ . The third and fourth terms denote the frictional pressure loss in the two-phase water–solid flow and in the three-phase flow. The fifth and sixth terms denote the weight of the two-phase water–solid mixture and that of the three-phase mixture. The seventh term denotes the hydrostatic pressure force of the surrounding water, acting on the bottom end of the pipe at section  $E$ . The pressure at  $O$  is assumed to be equal to atmospheric pressure. It is noted that, the interaction forces between the phases such as drag and virtual mass forces appear in the mathematical formulation only if the conservation equations of mass and momentum are applied for each phase separately.

Here, the mean velocity of any phase " $y$ " ( $y$  may be an air, liquid or solid phase) is given by  $u_y = \frac{j_y}{\epsilon_y}$

The first and second terms on the left-hand side of Eqn. (1), may be rewritten as follows:

$$A\{\rho_L j_L u_{L,E} + \rho_S j_S u_{S,E}\} = A\rho_{PS} j_{PS,E} u_{PS,E} \quad (2)$$

$$A\{\rho_{G,O} j_{G,O} u_{G,O} + \rho_L j_{L,O} u_{L,O} + \rho_S j_{S,O} u_{S,O}\} = A\{\rho_{G,O} j_{G,O} u_{G,O} + \rho_{PS,O} j_{PS,O} u_{PS,O}\} \quad (3)$$

where  $PS$  denotes a pseudoliquid which is formed by liquid and solid phase, i.e. treating a two-phase flow as a single phase as pseudoliquid.

where  $j_{ps}$ ,  $\rho_{ps}$  and  $u_{ps}$  are the volumetric flux, density and mean velocity for pseudoliquid at section  $E$  respectively. These are expressed as:

$$j_{PS,E} = j_{L,E} + j_{S,E} \quad \text{and}$$

$$\rho_{PS,E} = \epsilon_{L,E} \rho_L + \epsilon_{S,E} \rho_S$$

where  $\epsilon_{L,E}$  and  $\epsilon_{S,E}$  are void fractions for liquid and solid at section  $E$ ,

respectively, and  $\rho_L$  and  $\rho_S$  are liquid and solid density respectively. The third term on the left-hand side of eqn. (1) may be rewritten as follows:

$$\pi D \int_E^I \tau_{PS} dz = A \left\{ \frac{\Delta P_{f,PS}}{\Delta z} L_2 + \Delta P_E \right\} \quad (4)$$

where  $\Delta P_{f,PS}/\Delta z$  is the frictional pressure gradient in two-phase water solid flow and  $\Delta P_E$  is the entrance pressure drop of the suction pipe, which is the sum of the entrance fitting loss and the entrance length loss, occurs at  $E$ .

Since both the air pressure and air flow rate vary throughout the air-lift pump, the frictional pressure gradient in the three-phase flow cannot be estimated at the middle of the upriser tube and, therefore, the upriser tube should be divided into  $N$  segments in the flow direction as shown in Fig. (1). The length of each segment is chosen such that the nodes length, for the segment ( $k$ ) is the same for every segment. The frictional pressure loss term in the momentum equation is then calculated using step-by-step integration procedure for  $N$  steps as follows:

Assuming that the pressure distribution for each segment is linear, and the frictional pressure gradient of each segment is calculated at the middle of this segment. The fourth term on the left-hand side of eqn. (1) can be rewritten as:

$$\pi D \int_I^O \tau_f dz = A \left\{ \sum_{k=1}^n \frac{\Delta P_{f,3}(K)}{\Delta z(K)} \Delta z(K) + \Delta P_I \right\} \quad (5)$$

where  $\Delta P_{f,3}(k)/\Delta z(k)$  is the frictional pressure gradient in the three-phase flow at the  $k^{th}$  node, and  $\Delta P_I$  is the entrance pressure drop of the upriser tube, occurs at section I.



The fifth term on the left-hand side of eqn. (1)

$$A \int_B (\rho_L \varepsilon_{L,PS} + \rho_S \varepsilon_{S,PS}) g dz = A g \rho_{PS,B} L_2 \quad (6)$$

The gravity force of the three-phase mixture (air and pseudoliquid phase).

The sixth term on the left-hand side of the momentum eqn. (1), is estimated in the same way as the pressure gradient and is rewritten as:

$$\begin{aligned} & A \int_I (\rho_G \varepsilon_G + \rho_L \varepsilon_{L,3} + \rho_S \varepsilon_{S,3}) g dz \\ &= A \int_I (\rho_G \varepsilon_G + \rho_{PS,3} \varepsilon_{PS,3}) g dz \\ &= A g \sum_{k=1}^N (\varepsilon_G(k) \rho_G(k) + \rho_{PS,3} \varepsilon_{PS,3}(k)) \Delta z(k) \quad (7) \end{aligned}$$

### 2.1.2 Correlations of volumetric fractions

The correlations of volumetric fractions in eqs. (2) to (7) are obtained from the following correlations.

#### (a) Volumetric fraction of solid particles

The volumetric fraction  $\varepsilon_{S,PS}$  of solid particles in a two-phase flow (single phase pseudoliquid flow) is expressed as:

$$\varepsilon_{S,PS} = \frac{j_{S,PS}}{u_{S,PS}} \quad (8)$$

Similarly, the volumetric fraction,  $\varepsilon_{S,3}$ , of solid particles in a three-phase flow (two-phase pseudoliquid flow) is expressed as:

$$\varepsilon_{S,3} = \frac{j_{S,3}}{u_{S,3}} \quad (9)$$

where  $u_{S,3}$  and  $u_{S,PS}$  are the velocities of solid particle in two-phase and in three-phase flow. These velocities are according to Wallis (1969) as:

$$u_{S,PS} = C_1(j_S + j_L) + C_2 u_{ST} \quad (10)$$

and

$$u_{S,3} = C_1(j_S + j_L + j_G) + C_2 u_{ST} \quad (11)$$

where  $C_1$  and  $C_2$  are the distribution coefficients for a spherical particles.

The values  $C_1$  of and  $C_2$  are 1.2 and 1, respectively, (Zuber and Findlay (1965)).

The free settling velocity  $u_{ST}$  for a single particle in still water is expressed as:

$$u_{ST} = \sqrt{\frac{4}{3} \frac{g d_s}{C_{ds}} \left( \frac{\rho_S - \rho_L}{\rho_L} \right)} \quad (12)$$

where  $d_s$  is solid particle diameter and  $C_{ds}$  is the drag coefficient of solid particles and can be evaluated as a function of the particle Reynolds number, (Weber and Dedegil (1976)) as follows:

$$C_{ds} = \begin{cases} (24/Re_\infty)(1+0.15Re_\infty^{0.687}) & Re_\infty \leq 1000 \\ 0.44 & Re_\infty > 1000 \end{cases} \quad (13)$$

Here,  $Re_\infty$  is defined by

$$Re_\infty = \frac{d_s u_\infty \rho_L}{\mu_L}, \quad (14)$$

$$u_\infty = 0.345 \sqrt{gD}, \quad (15)$$

and

$$j_L + j_S = j_{PS}, \quad (16)$$

where  $D$  is pipe diameter and  $j_{PS}$  is the volumetric flux of the pseudoliquid and is given by

$$j_{PS} = \left( \frac{M_L + M_S}{A \rho_{PS,3}} \right) \quad (17)$$

where  $M_L$  and  $M_S$  are the mass flow rate for liquid and solid.

where  $\rho_{PS,3}$  is the mean density of the pseudoliquid in the three-phase mixture. It is expressed according to Yashinaga and Sato (1996) by the following expression:

$$\rho_{PS,3} = \rho_L \left( \frac{\varepsilon_{L,3}}{1 - \varepsilon_G(k)} \right) + \rho_S \left( \frac{\varepsilon_{S,3}}{1 - \varepsilon_G(k)} \right) \quad (18)$$

#### (b) Volumetric fraction of the air

The following relation expresses the air volumetric fraction in the three-phase flow which is modified as a two-

phase air-pseudoliquid flow

$$\epsilon_G = \frac{J_G}{C_o(J_{PS} + J_G) + \bar{u}_{sl}} \quad (19)$$

where  $C_o$  and  $\bar{u}_{sl}$  depend on the flow regime, and expressions used are given in Table (1), Wallis (1969).

Table (1) Constants  $C_o$  and  $\bar{u}_{sl}$  depend on the flow regimes, (Wallis (1969)).

| Flow Regime | $C_o$                                      | $\bar{u}_{sl}$   |
|-------------|--|--|
| Bubbly      | $(1.2 - 0.2 \sqrt{\frac{\rho_G}{\rho_L}})$ | $1.4 \left[ \frac{\sigma g (\rho_L - \rho_G)}{\rho_L^2} \right]^{1/4}$ |
| Slug        | 1.2  | $0.35 \left[ \frac{g (\rho_L - \rho_G) D}{\rho_L} \right]^{1/2}$       |
| Churn       | 1.0-1.3                                    | $0.35 \left[ \frac{g (\rho_L - \rho_G) D}{\rho_L} \right]^{1/2}$       |
| Annular     | 1.0-1.1                                    | $0.32 \left[ \frac{\sigma g \rho_L - \rho_G}{\rho_G^2} \right]^{1/4}$  |

(c) Volumetric fraction of the water

By knowing the volumetric fraction of solid particles and gas, the liquid volumetric fractions,  $\epsilon_{L,3}$ , is easily predicted by the following relation:

$$\epsilon_{L,3} = 1 - \epsilon_G - \epsilon_{s,3} \quad (20)$$

2.1.3 Correlations of friction pressure drops

The correlations of friction pressure drop in eqs. (4) and (5) are obtained from the following correlations:

(a) Frictional pressure drop in the two-phase water-solid flow

$\Delta P_{f,PS} / \Delta z$  Frictional pressure drop in the water-solid two-phase flow (pseudoliquid) in Eqn. (4) is obtained from the following correlation

$$\frac{\Delta P_{f,PS}}{\Delta z} = \lambda_{PS} \frac{\rho_{PS}}{2D} j_{PS}^2 \quad (21)$$

The friction coefficient in equation (21) for hydraulically smooth and rough pipes can be calculated

according to Blasius formula and is given by

$$\lambda_{ps} = 0.316 Re_{ps}^{-0.25} \quad (\text{Smooth pipe}) \quad (22)$$

$$\lambda_{ps} = 1.8 \left[ \log_{10} \frac{Re_{ps}}{0.135 \left( Re_{ps} \frac{\alpha}{D} \right) + 6.5} \right] \quad (\text{Rough pipe}) \quad (23)$$

where  $\alpha$  is the mean pipe roughness. equation (23) was modified by Round and Garg (1986). It is valid for  $0 \leq \alpha / D \leq 0.005$  and  $4000 \leq Re \leq 10^8$ . The Reynolds number ( $Re_{ps}$ ) is defined as:

$$Re_{ps} = \frac{u_{ps} D}{\nu_{ps}}, \quad (24)$$

where  $u_{ps}$ ,  $\nu_{ps}$  velocity and kinematic viscosity of pseudoliquid.

The kinematics viscosity,  $\nu_{ps}$ , is modified as:

$$v_{PS} = \frac{\mu_{PS}}{\rho_{PS}} = \left( \frac{\rho_{PS} - \rho_s \epsilon_s}{\rho_{PS}} \right) v_L \quad (25)$$

where  $v_L$  is the kinematics viscosity of the liquid.

### (b) Entrance pressure drop in the two-phase water-solid flow

$\Delta P_E$  in equation (4) accounts for both pressure drop by the inlet flow, which depends on the shape of the inlet fitting and also for pressure drop due to the acceleration of the slurry from standstill to the mean flow velocity in the suction tube. It is calculated according to Dedegil's equation (1986):

$$\Delta P_E = (\zeta + \zeta_E) \frac{\rho_{PS}}{2} j_{PS}^2 \quad (26)$$

where  $\zeta$  is the coefficient of inlet fitting loss was set equal to 0.5, and  $\zeta_E$  is the coefficient of the entrance length loss was set equal to 1 according to Dedegil (1986).

### (c) Frictional pressure drop in the three-phase flow

Regarding the three-phase flow a two-phase air-pseudoliquid flow, the frictional pressure gradient in the three-phase flow corresponding to the  $k^{\text{th}}$  segment may be found from the following relations, (Chishlom and Laird (1958)),

$$\frac{\left\{ \frac{\Delta P_{f,3}(k)}{\Delta z(k)} \right\}}{\left\{ \frac{\Delta P_{f,ps}}{\Delta z} \right\}} = 1 + \frac{21}{\chi} + \frac{1}{\chi^2} \quad (27)$$

Where

$$\chi^2 = \frac{\left\{ \frac{\Delta P_{f,ps}}{\Delta z} \right\}}{\left\{ \frac{\Delta P_{f,g}}{\Delta z} \right\}} \quad (28)$$

The gas friction term is obtained as follows:

$$\frac{\Delta P_{f,g}}{\Delta z} = 0.5 \frac{\lambda_G \rho_G j_G^2}{D} \quad (29)$$

The gas friction coefficient  $\lambda_G$  is given as:

$$\lambda_G = 0.312 Re_G^{-0.25} \quad (30)$$

$Re_G$  is the gas Reynolds number and defined as:

$$Re_G = \frac{\rho_G D j_G}{\mu_G} \quad (31)$$

### (d) Entrance length loss in the three-phase flow

The pressure drop would  $\Delta P_i$  in equation (5) caused by the acceleration of the two-phase water-solid mixture due to air injection, may be defined according to Dedegil (1986), injecting the kinematic energy of the injecting air in the flow direction, as follows:

$$\Delta P_i = \zeta_i \left[ \frac{\rho_{PS,3}}{2} \left( \frac{j_{PS}}{1 - \epsilon_{G,3}} \right)^2 - \frac{\rho_{PS}}{2} j_{PS}^2 \right] \quad (32)$$

where the coefficient,  $\zeta_i$ , was set equal to 1. It is apparent that equation (32) expresses the difference in kinetic energy of the pseudoliquid upstream and down stream of the air injection level.

## 2.2. Air-Lift Pump Efficiency

The power consumed due to the gas compression from atmospheric pressure to the air injection pressure, assuming isothermal comparison, is given by the following equation:

$$\begin{aligned} N_C &= M_G RT \ln \left( \frac{P_i}{P_0} \right) \\ &= \rho_0 A J_{G,0} \ln \left( \frac{P_i}{P_0} \right) \end{aligned} \quad (33)$$

where  $P_0$ ,  $P_i$ ,  $R$ , and  $T$  are the pressure at pump outlet equals to atmospheric pressure, the absolute pressure of the

injected air ( $= P_{(i)} + \Delta P_i$ ), gas constant and absolute temperature of the gas phase, respectively.

The power gained is then given by the following general relation:

$$N_G = C \{ g(L_1 + L_2) A \rho_i j_i - \rho_l g(L_2 + L_3) A j_l \} + (1-C) [\rho_l A j_l g(L_1 - L_3)] \quad (34)$$

where  $C = 0$  when lifting liquids and  $C = 1$  while pumping solids.

Therefore, the theoretical lifting efficiency is calculated according to the following equation:

$$\eta_{th} = \frac{N_G}{N_C} \quad (35)$$

To take into account the slip between the particles and the phases throughout the whole lifting pipe, an additional efficiency term called slip efficiency ( $\eta_s$ ) should be concerned. It is defined according to Boes et al. (1972), while for the whole air-lift tube (concerning the N segments, air injection section, outlet section, and the two-phase flow section) as:

$$\eta_s = 1 - \frac{1}{N+3} \sum \frac{u_{st}}{j_G + j_L + j_S} \quad (36)$$

where  $u_{st}$  is the free settling velocity of the particles.

Finally, if the loss of hydraulic energy in the air compressor, inclusive air conduit losses, is concerned in an efficiency term called compressor efficiency ( $\eta_c$ ) therefore the air-lift pump overall or total efficiency ( $\eta_p$ ) is defined as:

$$\eta_p = \eta_{th} \eta_s \eta_c \quad (37)$$

### 2.3 Empirical Correlation for Liquid Volumetric Flux and Pump Parameters

Most of the previous published models used two variables as the input values to the program. The two variables are volumetric flux of gas ( $j_G$ ) and the volumetric flux of liquid ( $j_L$ ). Added to these two variables, the volumetric flux of solid ( $j_S$ ) in case of three-phase flow. Using these variables as input values is not a good representation of real engineering case, where the air flow rate is the only input parameter and the output is both water and solid flow rates.

The liquid volumetric flux is dependent upon the operating and geometrical parameters. Therefore, an empirical relationship between the liquid volumetric flux and the operating and geometrical parameters could be obtained from the experimental data which are available in literature. This empirical relation is used for estimating the volumetric flux of liquid ( $j_L$ ) as a first iteration. The experimental data of Yoshinaga and Sato (1996) and Fujimoto et al. (2003) are used to find the empirical correlation.

The correlation could be defined by an equation of the type:

$$j_L = (0.0995858) j_G^{(0.195665)} S_r^{(1.2666)} (\rho_s d_s^3)^{(0.02747)} D^{(-0.01681)} \quad (38)$$

The mean percentage error for the correlation is 23.8 %.

### 3. MODEL VALIDATION

Validation of the theoretical model is an important aspect developing any code program. Therefore, the computational results are compared with published extensive experimental results in Yoshinaga and Sato (1996) and Fujimoto et al. (2003).

For each set of published experimental data, the mean error has been examined.

The mean error results are shown in Table (2)

Table (2) Mean error (D = 26 mm)

| Experimental results        | Yoshinaga and Sato (1996) |       |     |       | Fujimoto et al. (2003) |
|-----------------------------|---------------------------|-------|-----|-------|------------------------|
|                             | 0                         | 0.025 | 0   | 0.045 | 0.008                  |
| Solid volumetric flux (m/s) | 0.7                       | 0.7   | 0.8 | 0.8   | 0.675                  |
| Submergence ratio, %        | 11.3                      | 7.7   | 14  | 8.2   | 6                      |

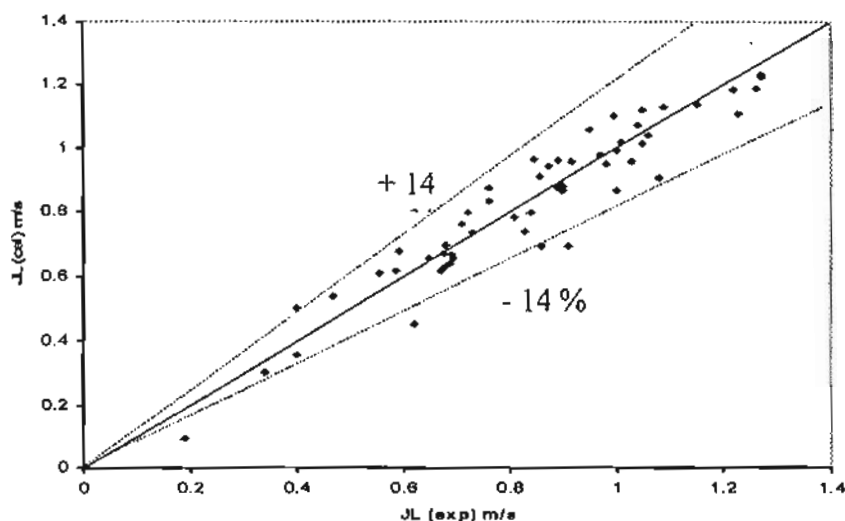


Fig. (2): The deviations between the present predicted results and the published results (Yoshinaga and Sato (1996) and Fujimoto et al. (2003)) for water volumetric flux.

Figure (2) indicates that the agreement is good and most points fall within  $\pm 14\%$  lines.

#### 4. RESULTS AND DISCUSSIONS

The proposed model is verified by comparing the theoretical results with the published data. Therefore, the calculations can be safely extended to study and discuss the effect of different operational parameters on the air-lift pump performance. The predicted results are indicated; the air-lift pump performance with gas volumetric flux, solid particles density, solid particle diameter, and solid volumetric flux. An iterative solution is required for the calculation of liquid volumetric flux and also for the other parameters

involved in the momentum equation (1). During the calculations, the gas temperature at the injection point is assumed the same as the temperature of the liquid–solid mixture (i.e. the phases are in thermal equilibrium). Moreover, the temperature gradient is neglected through the riser tube. Therefore, an isothermal expansion of gas from inject pressure,  $P_i$ , to pump outlet pressure,  $P_o$  (equal to atmosphere pressure), may be held.

##### 4.1 Effect of Air Volumetric Flux, $J_G$

The most significant operating parameter is the air volumetric flux which has a great effect on both water volumetric flux and efficiency of the air-lift pump. The air volumetric flux

was ranged between 0.5 to 12 m/s in this study. The effect of the air volumetric flux on the water volumetric flux (i.e. pump discharge), at different submergence ratios, solid volumetric fluxes and solid particle diameters at constant diameter of the upriser is shown in Figures (3) to (5). From these Figures it is observed that an increase in the air volumetric flux initially causes the water volumetric flux to increase gradually reaching its maximum value, when the air volumetric flux is between 2 to 4 m/s, then slightly decreased with increasing the air volumetric flux. The air volumetric flux corresponds to the maximum water volumetric flux is the optimum air volumetric flux where the flow pattern is mainly slug-churn flow. The optimum air volumetric flux is inversely proportional to the submergence ratio at a constant pipe diameter. It is known that the air-lift pump works on the density difference principle where the density of the mixture is varying and the density of the liquid remains constant. Increasing the air volumetric flux, a greater quantity of pressurized air from the injection holes will mix with water, resulting in a decrease in the mixture's density, which leads to a gain in the kinetic head. This is ultimately results in an increase in the discharge of water, because the raising of liquid has been found to be mainly due to kinetic head. An increase in the air volumetric flux beyond the optimum values causes a drop in the water volumetric flux. This may be attributed to the flow

transition from slug flow to churn flow or annular flow. At lower air volumetric flux, bubbly flow regime doming in the upriser tube, while at higher air volumetric flux the flow pattern tends to become churn or annular.

Figures (6) to (8) show the variation of pump efficiency with air-volumetric flux. From these figures we have observed that, for constant pipe diameter and for different submergence ratios. The efficiency increases sharply with increasing the air volumetric flux. until limited points (depending on the submergence ratio), where the efficiency reaches its maximum value at air volumetric flux between 0.5 to 2 m/s. Further increase in air volumetric flux will cause a significant decrease in the efficiency. It could be attributed to the fact that the flow pattern in the upriser tube at higher air volumetric flux tends to become churn or annular. At lower air volumetric flux, slug flow is dominated in the air-lift tube. In this flow regime, the efficiency is directly proportional to the air volumetric flux. The results for all submergence ratios, solid volumetric fluxes and solid particle diameters indicate the same common pattern of variation. It is clear from Figures (3) to (8) that the values of air volumetric flux at which maximum values of water volumetric flux occur are higher than that at which maximum efficiencies occur. Therefore, operating the pump should be between the two values of maximum water volumetric flux and maximum efficiency.

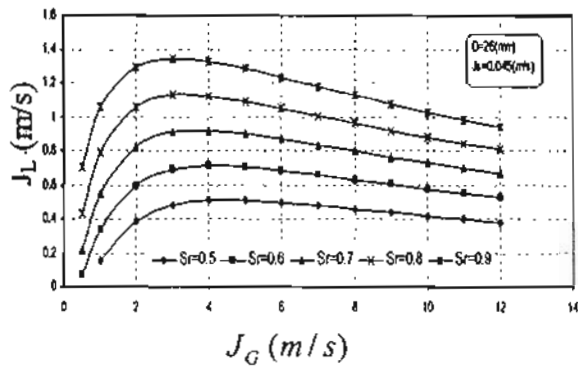


Fig. (3): Variation of liquid volumetric flux with gas volumetric flux at various submergence ratios ( $d_s = 6.12$  mm).

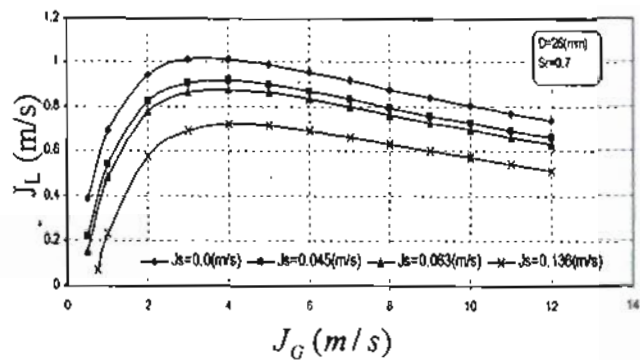


Fig. (4): Variation of liquid volumetric flux with gas volumetric flux at various values of solid volumetric flux ( $d_s = 6.12$  mm).

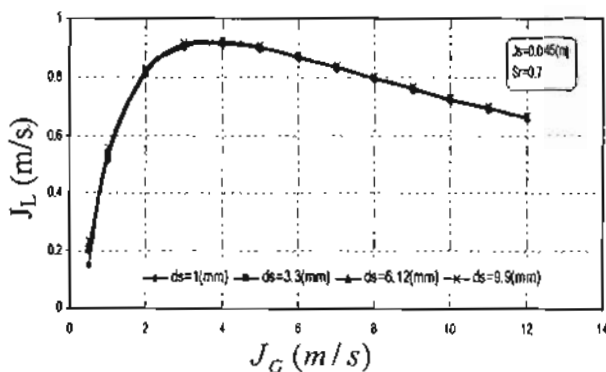


Fig. (5): Variation of liquid volumetric flux with gas volumetric flux at various values of solid particles diameter ( $D = 26$  mm).

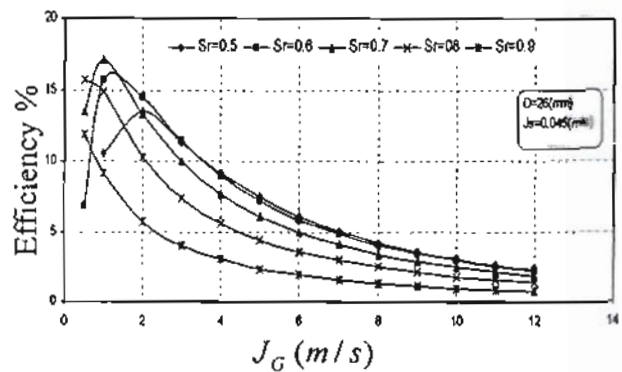


Fig. (6): Variation of efficiency with gas volumetric flux at various submergence ratios ( $d_s = 6.12$  mm).

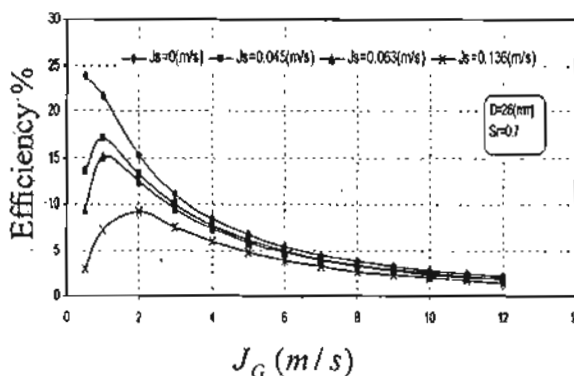


Fig. (7): Variation of efficiency with gas volumetric flux at various values of solid volumetric flux ( $d_s = 6.12$  mm).

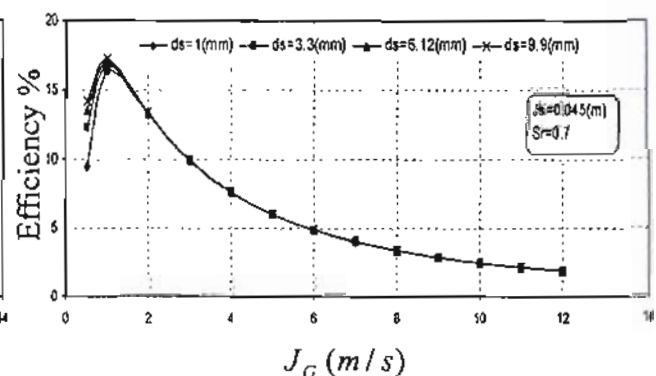


Fig. (8): Variation of efficiency with gas volumetric flux at various values of solid particles diameter ( $D=26$  mm).

### 4.2 Effect of Solid Volumetric Flux, $J_s$

The performance of the air-lift pump is predicted theoretically for solid particles volumetric flux values ranged from zero (two-phase flow) to 0.1 m/s at different values of air volumetric flux, submergence ratio and solid particles diameters. Figures (9) to (14) show the variation of water volumetric flux and pump efficiency with solid volumetric flux. The results for all conditions indicate a common pattern of variation. Generally, these

Figures illustrate that both the water volumetric flux and efficiency decrease linearly with increasing the solid particles volumetric flux. This behavior may be interpreted as follows: as the solid volumetric flux increases, the mean velocity of flow increases also. The increasing in the mean velocity of the flow causes an increase in the head losses and subsequently both water volumetric flux and efficiency of the air- lift pump decreases.

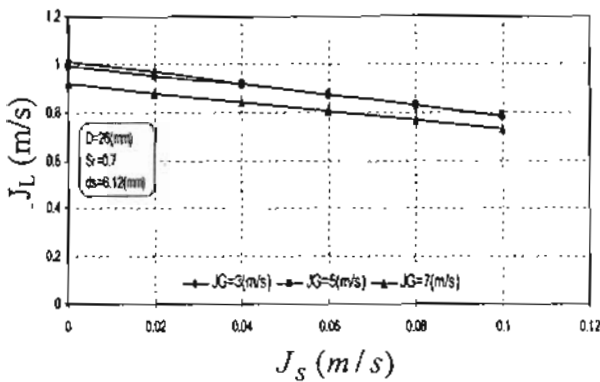


Fig. (9): Variation of liquid volumetric flux with solid volumetric flux at various values of gas volumetric flux.

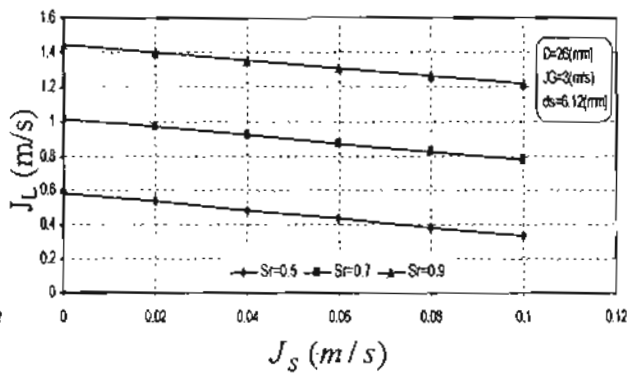


Fig. (10): Variation of liquid volumetric flux with solid volumetric flux at various submergence ratios.

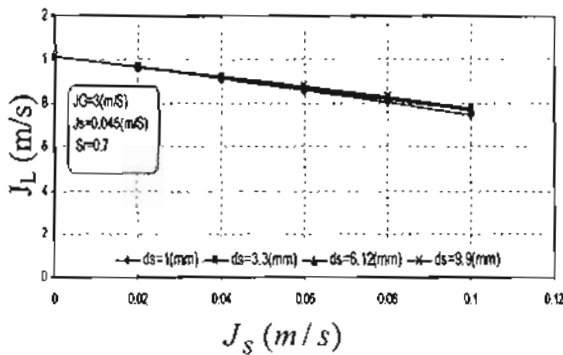


Fig (11): Variation of liquid volumetric flux with solid volumetric flux at various values of solid particles diameter ( $D=26\text{mm}$ ).

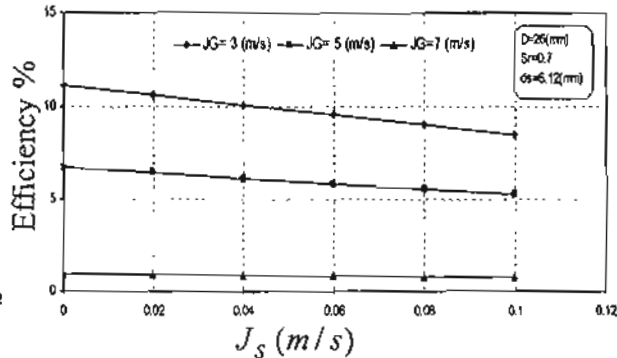


Fig. (12): Variation of efficiency with solid volumetric flux at various values of gas volumetric flux .



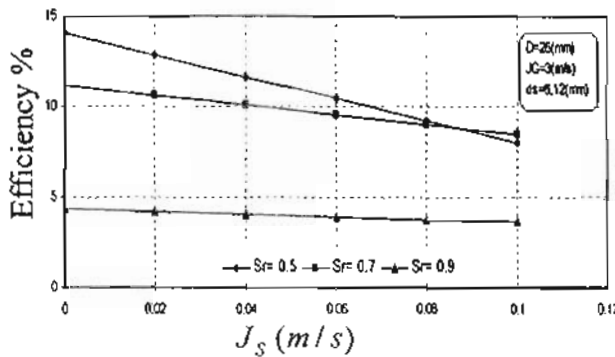


Fig. (13): Variation of efficiency with solid volumetric flux at various submergence ratios.

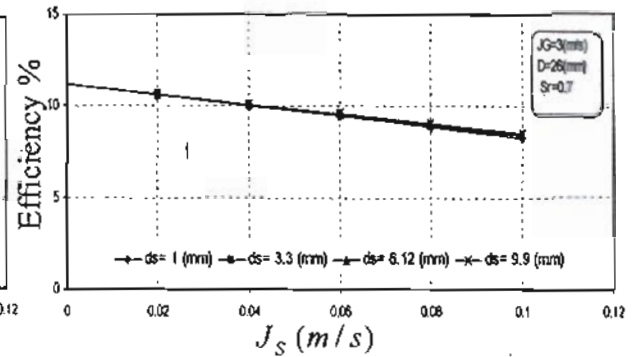


Fig. (14): Variation of efficiency with solid volumetric flux at various values of solid particles diameter.

### 4.3 Effect of Solid Particles Density, $\rho_s$

The effects of solid particles density on the performance of an air-lift pump operating at various conditions are illustrated in Figures (15) to (20). It can be seen clearly from these figures that, as the solid particles density increases from 1000 to 4000 kg/m<sup>3</sup>, under otherwise constant conditions, the water volumetric flux and the air-lift pump efficiency are decreased linearly. These observations may be attributed to the settling velocity of solid particles, defined by equation (12), which increases with increasing the density of solid particles. For particles with high settling velocity, greater water

velocities are needed to initiate lifting of solids and thus higher air volumetric fluxes are needed. The drop in the total pressure owing to the weight of the mixture increases at higher settling velocities where the solid particles cause higher volumetric concentration in the cross-sectional area of the pipe, higher solid-liquid mixture density ( $\rho_s$ ) and higher pressure gradients due to their lower absolute velocity. Increasing the total pressure loss in the suction pipe tends to decrease the air injection pressure. The combinations of these factors may cause a decrease in the water volumetric flux and efficiency with increasing the solid-particles density.

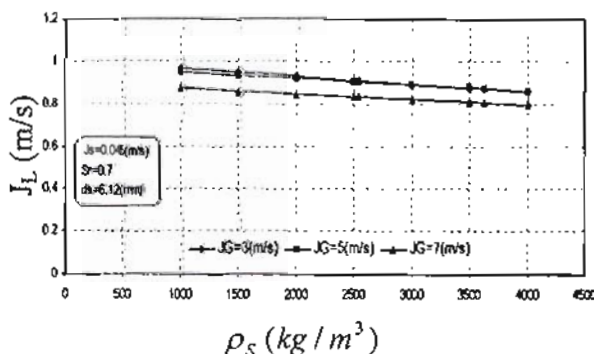


Fig. (15): Variation of liquid volumetric flux with solid particles density at various values of gas volumetric flux (D=26 mm).

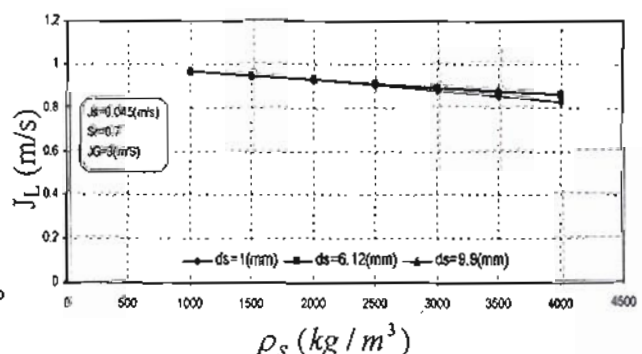


Fig. (16): Variation of liquid volumetric flux with solid particles density at various values of solid particles diameter (D=26mm).

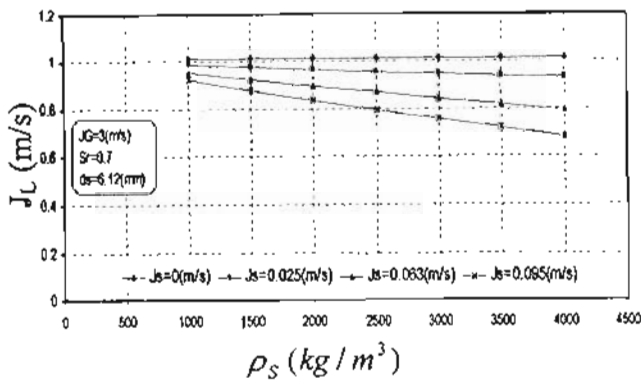


Fig. (17): Variation of liquid volumetric flux with solid particles density at various values of solid volumetric flux (D=26 mm).

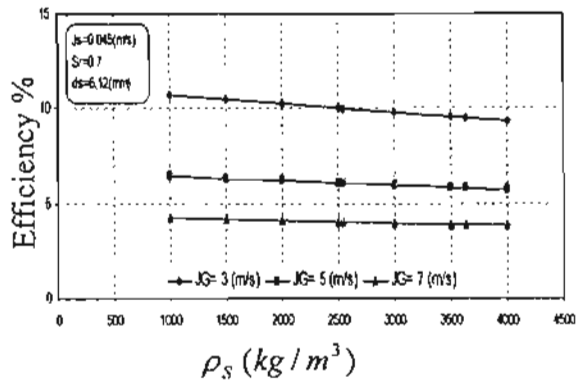


Fig. (18): Variation of efficiency with solid particles density at various values of gas volumetric flux (D=26 mm).

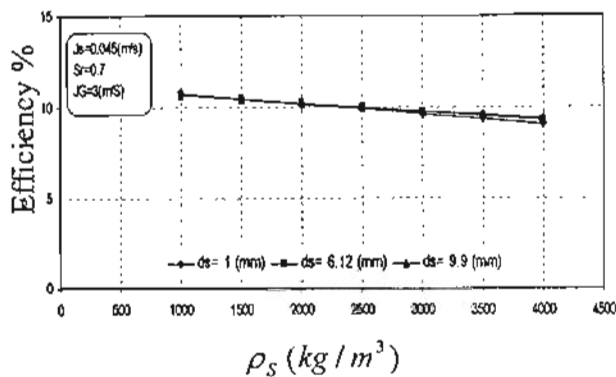


Fig. (19): Variation of efficiency with solid particles density at various values of solid particles diameter (D=26 mm).

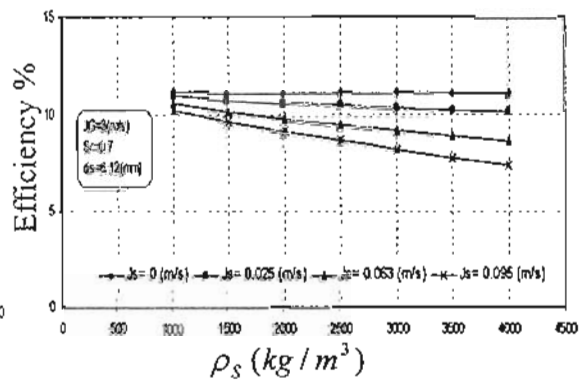


Fig. (20): Variation of efficiency with solid particles density at various values of solid volumetric flux (D = 26 mm).

#### 4.4 Effect of Solid Particles Diameter, $d_s$

The influence of solid particles diameter on the lifting characteristics of an air-lift pump is shown in Figures (21) to (26). These figures show that the diameter of the solid particles has insignificant effect on the water volumetric flux and efficiency through the studied range from 2 to 10 mm. Due to increasing the diameter of the solid particles with  $J_s$  constant, the free settling velocity is increased also. This

yields an increase in the slip between the particles and the mean flow. Also, the force needed in lifting particles is much greater for particles with large diameter than that with small one. In addition, increasing the diameter of the solid particles at a constant solid volumetric flux decreases the number of solid particles within the flow. Therefore, the combination of these three factors may cause unchanged in the water volumetric flux and pump efficiency.

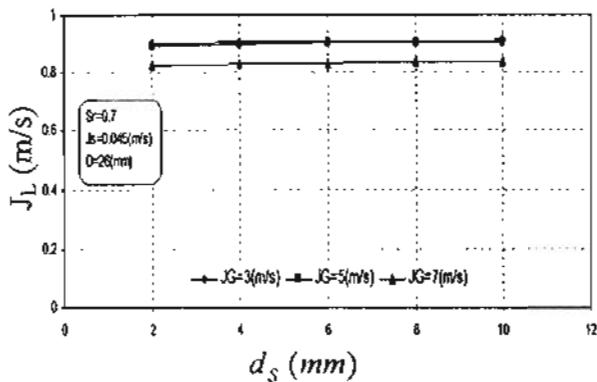


Fig. (21): Variation of liquid volumetric flux with solid particles diameter at various values of gas volumetric flux.

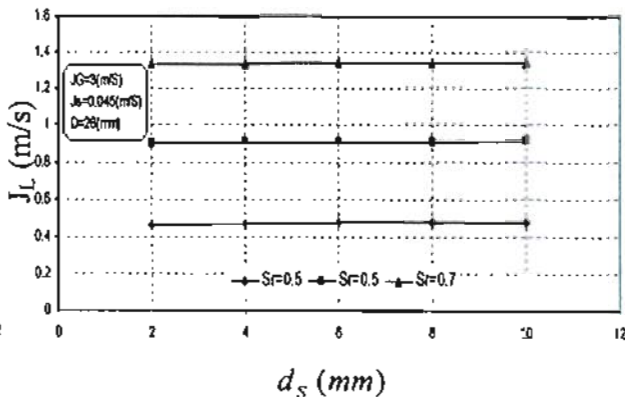


Fig. (22): Variation of liquid volumetric flux with solid particles diameter at various submergence ratios.

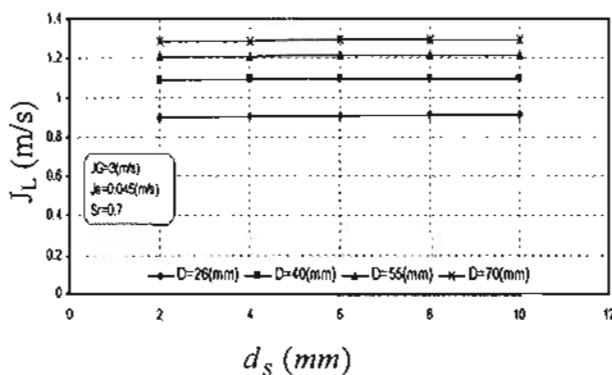


Fig. (23): Variation of liquid volumetric flux with solid particles diameter at various values of pipe diameter.

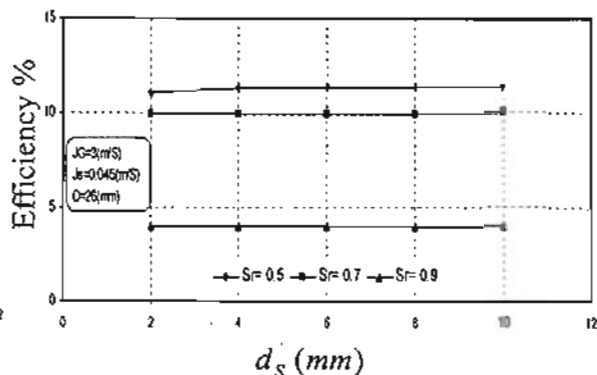


Fig. (24): Variation of efficiency with solid particles diameter at various values of gas volumetric flux.

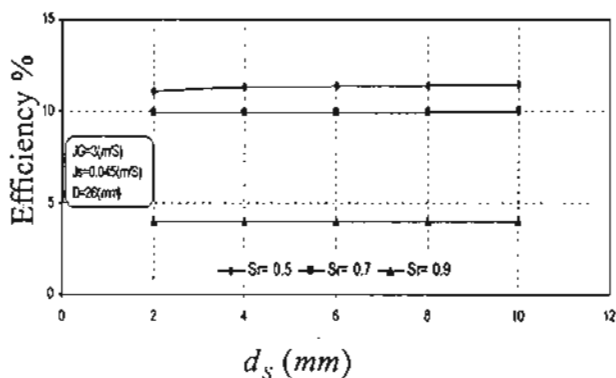


Fig. (25): Variation of efficiency with solid particles diameter at various submergence ratios.

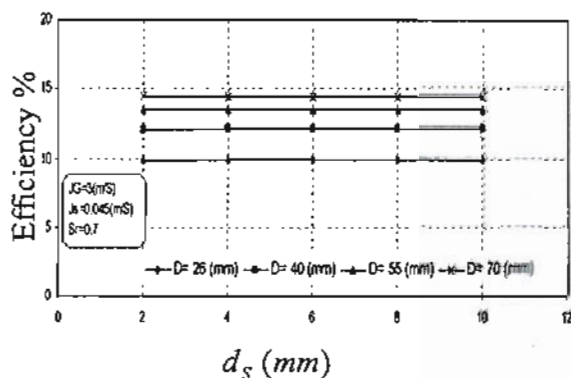


Fig. (26): Variation of efficiency with solid particles diameter at various values of pipe diameter.

## CONCLUSIONS

The effects of operational parameters on the performance of an air-lift pump were investigated theoretically, based on the results obtained; the following conclusions can be drawn:

1. The proposed model is suitable for predicting the performance of air-lift pump operated with two-phase flow (liquid and gas) or three-phase flow (liquid, solid and gas).
2. Comparison between the predicted performance (water volumetric flux and pump efficiency) using the present model and the

published experiments results showed a good agreement.

3. The results showed that the water volumetric flux and pump efficiency increase gradually to maximum value some where it was between 1 to 4  $m/s$ , then slightly decrease with increasing air volumetric flux.
4. The water volumetric flux and pump efficiency decrease linearly with increasing the solid particles volumetric flux.
5. Solid particles density and diameter had no significant effects on the pump performance.

## NOMENCLATURE

|  |   |
|--|---|
| $A$ Pipe cross sectional area ( $m^2$ )      | $J$ Volumetric flux ( $m/s$ )   |
| $C$ Distribution coefficient                 | $L_1$ Length of upriser between the air injection ports and discharge ports ( $m$ ) |
| $C_{ds}$ Drag coefficient of solid particles | $L_2$ Length of suction pipe (two-phase flow) ( $m$ )                               |
| $d_s$ Diameter of solid particles ( $m$ )    | $L_3$ Length of upriser between the air injection ports and the water level ( $m$ ) |
| $D$ Pipe diameter ( $m$ )                    | $M$ Mass flow rate ( $kg/s$ )   |
| $g$ Gravitational acceleration ( $m/s^2$ )   | $N$ Number of cells   |
| $P$ Pressure ( $N/m^2$ )                     | $N_C$ Power consumed ( $W$ )  |
| $Q$ volume flow rate ( $m^3/s$ )             | $N_G$ Power gained ( $W$ )  |
| $R$ Universal gas constant ( $J/kg.K$ )      | $u$ Velocity ( $m/s$ )  |
| $Re$ Reynolds number                         | $y$ Quality   |
| $Sr$ Submergence ratio %                     | $T$ Temperature ( $K$ )   |

### Greek letters

|  |  |
|--|--|
| $\nu$ Kinematics viscosity ( $m^2/s$ ) | $\epsilon$ Void fraction (volumetric fraction) |
| $\lambda$ Friction factor              | $\rho$ Density ( $kg/m^3$ )                    |
| $\tau$ Shear stress ( $N/m^2$ )        | $\sigma$ Surface tension ( $N/m$ )             |
| $\zeta$ Entrance pressure loss factor  | $\eta$ Efficiency of the pump                  |
| $\alpha$ Mean pipe roughness           | $\mu$ Fluid viscosity ( $N.s/m^2$ )            |

### Subscripts

|                               |                               |
|-------------------------------|-------------------------------|
| $f$ friction                  | $PS$ Liquid-Solid             |
| $G$ Gas                       | $m$ Mixture                   |
| $L$ Liquid                    | $Go$ Gas at the pressure $Po$ |
| $S$ Solid                     | $3$ Three-phase flow          |
| $K$ Property at cell face $k$ |                               |

## REFERENCES

- Abed, K. A., 2003. Operational Criteria of Performance of Airlift Pumps, IE(I) Journal-MC, vol. 84.
- Awari, G.K., Ardhapurkar, P.M., Wakde, D.G., Bhuyar, L.B., 2004. Performance analysis of air-lift pump design, Proc. IMECH E Part C: J. Mech. Eng. Sci. 218, pp.1155-1161.
- Boës, Chr., During, R. and Wasserroth, E., 1972. Air-lift as a Drive for Single and Double Pipe Conveying Plants, *Fordern and Heben*, Vol. 22, No. 7, PP. 367-378.
- Brown, N. P. and Heywood, N. I., 1991. *Slurry Handling: Design of Solid-Liquid System*, London, New York, Elsevier Applied Science.
- Chisholm, D. and Laird, A., D., K., 1958. Two-Phase Flow in Rough Tubes, *Trans. ASME* 80, 276-286.
- Clark, N.N., 1984a. *Air Lift Pumps for Hydraulic Transport of Solids*, Powder Advisory Centre, London, 13-17.
- Clark, N. N., 1985. Predicting Holdup in Two-Phase Bubble Upflow and Downflow Using the Zuber and Findlay Drift-Flux model," *AIChE J.*, 31, 500.
- Clark, N. N., Dabolt, R. J., 1986. A General Design Equation for Airlift Pumps Operating in Slug Flow. *AIChE Journal*, vol. 32, pp.56-64.
- Dedegil, M.Y., 1986. Principles of Air-Lift Techniques, *Encyclopedia of Fluid Mechanics* (Edited by Chereimisinoff, N.P.), Vol. 4, Chapter 12, Gulf, Houston, TX.
- Fujimoto, H., Ogawa, S., Takuda, H. and Hatta, N., 2003. Operation Performance of a Small Air-Lift Pump for Conveying Solid Particles, *Journal of Energy Resources Technology*, ASME, vol.125, pp.17-25.
- Fujimoto, H., Murakami, S., Omura, A., and Takuda, H., 2004. Effect of Local Pipe Bends on Pump Performance of a small Air-lift system in transporting solid particles, *Int. J. of Heat & Fluid Flow*, vol. 25, PP.996-1005.
- Hatta, N., Fujimoto, H., Isobe, M. and Kang, J., 1998. Theoretical Analysis of Flow Characteristics of Multiphase Mixtures in a Vertical Pipe, *Int. J. Multiphase Flow* Vol. 24, No. 4, pp. 539-561.
- Imrich, K. J., Smith, M. S. and Bickford, D. F., 2004. *DWPF Air Lift Pump Life Cycle Evaluation (U)*, Savannah River Technology Center, U. S. Department of Energy.
- Kandil, H.A., Elmiligui, A.A., 1998. Experimental study of an Air Lift Pump Lifting Irregular Solid Particles, *Alexandria Eng. J.*, vol 37, A35-A43.
- Kato, H., Miyazawa, T., Tiyama, S., and Iwasaki, T., 1975. A Study of an Air-Lift Pump for Solid Particles, *Bull. JSME*, vol.18, pp. 286-294.
- Kassab, S.Z., Kandil, H.A., Warda, H.A., Ahmed, W.H., 2001. Performance of an Airlift Pump Operating in Multi-Phase Flow, *Proceedings of the 12th (IMPEC)*, vol. 1, Mansoura, Egypt, 2001, pp. F1-F13.
- Kassab, S.Z., Kandil, H. A., Warda, H.A. and Ahmed, W. H. 2007. Experimental and Analytical Investigations of Airlift Pumps Operating in three- Phase Flow, *Chemical Eng. J.*, vol. 131, pp.273-281.
- Khalil, M. F., Elshorbagy, K.A., Kassab, S.Z. and Fahmy, R.I., 1999. Effect of Air Injection Method on the Performance of an Air Lift Pump. *Journal of Heat and Fluid Flow*, vol. 20, pp. 598-604.

- Nicklin, D.J., 1963. The Air Lift Pump Theory and Optimization. ICHE 14, 29-39.
- Parker, G.J., 1980. The Effect of Foot Piece Design on the Performance of a Small Airlift Pump. Int. J. Heat & Fluid Flow. vol. 2, pp. 245-252.
- Round, G. F. and Garg, V. K., 1986. Applications of Fluid Dynamics, Published by E. Arnold, 403 pages.
- Stenning, A.H., Martin, C.B., 1968. An Analytical and Experimental Study of Air-Lift Pump Performance. J. Eng. Power Trans. ASME, vol. 4, pp.106-110.
- Wallis, G. B., 1969. One Dimensional Two-phase Flow, McGraw-Hill, New York.
- Weber, M., and Dedegil, M. Y., 1976. Transport of Solids According to the Air-Lift Principle, Proceedings of 4th International Conference on the Hydraulic Transport of Solids in Pipes, Alberta, Canada, H1-1-23 and X93-94.
- Wurts, w.A., McNeill, G. and Overhults, DG., 1994. Performance and Design Characteristics of Airlift pumps for Field Applications, Research Report, World Aquaculture 25 (4), 51-55.
- Yoshinaga, T., and Sato, Y., 1996. Performance of an Air-Lift Pump for Conveying Coarse Particles, Int. J. Multiphase Flow, 22, pp223-238.
- Zuber, N. and Findlay, J. A., 1965. Average Volumetric Concentration in Two-Phase Flow Systems, Trans. Am. Soc. Mech. Engrs, 87, Series C, PP. 453-468.